Electronic Supplementary Information

Studying NAD(P)H Cofactor-binding to Alcohol Dehydrogenases through Global Analysis of Circular Dichroism Spectra

Marija Marolt[1] and Steffen Lüdeke[1]

[1]*Institute of Pharmaceutical Sciences, Albert-Ludwigs-Universität Freiburg, Alberstr. 25, 79104 Freiburg, Germany*

Corresponding Author

PD Dr. Steffen Lüdeke
Institute of Pharmaceutical Sciences
Albertstr. 25, 79104 Freiburg
E-mail: steffen.luedeke@pharmazie.uni-freiburg.de
Tel.: +49 (0)761 203-67398
Fax: +49 (0)761 203-6351

Contents

I. Protein Purification

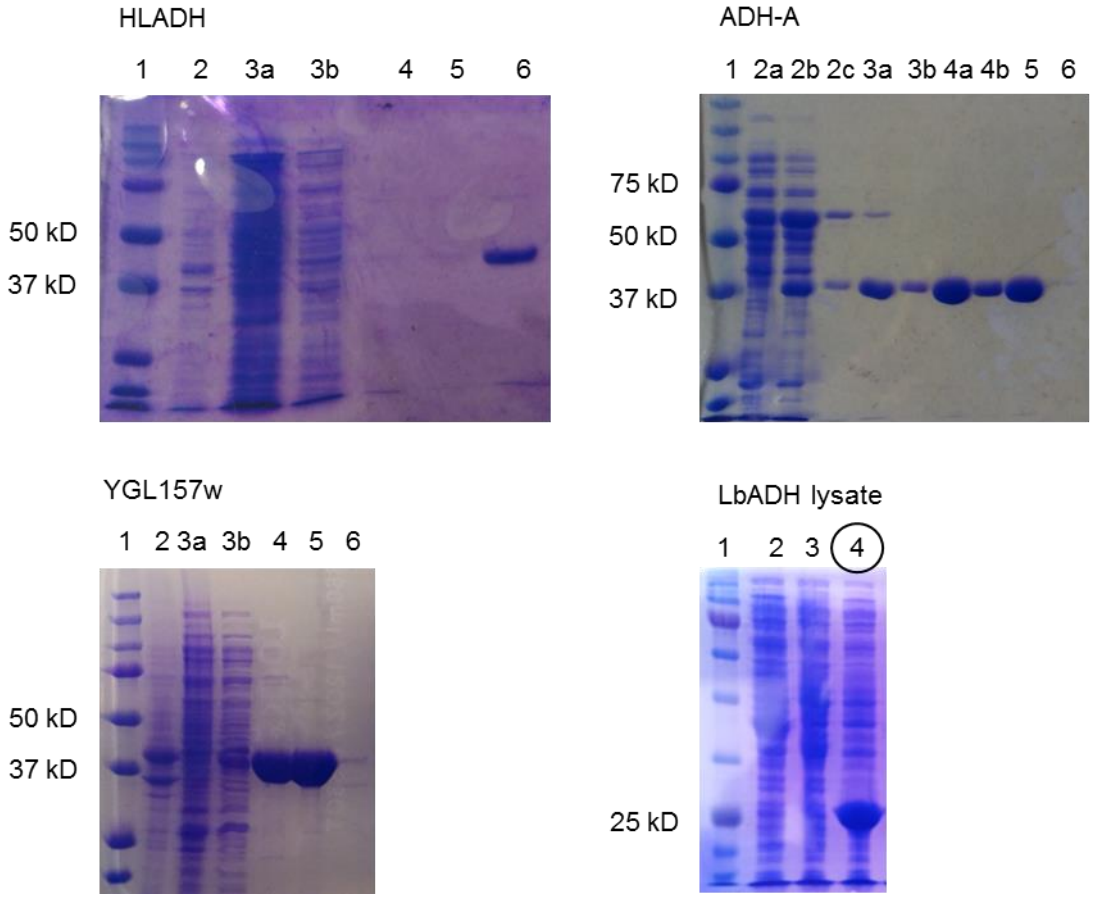

Figure S1. SDS-PAGE of HLADH, ADH-A and YGL157w after purification. Lane **1** shows Precision Plus Protein Prestained Dual Color marker (250 – 10 kD) (Bio-Rad, Munich, Germany). Except for 1 M, which was prepared in distilled H_2O, all imidazole solutions for the elution gradient were prepared in KPi buffer (50 mM, pH 7.5).

HLADH: cell pellet (**2**); 25 mM imidazole (**3a-b**); 100 mM imidazole (**4**); 1 M imidazole (**5**); HLADH (42 kD) collected in 500 mM imidazole KP buffer (**6**).

ADH-A: 25 mM imidazole (**2a-c**); 50 mM imidazole (**3a-b**); 100 mM imidazole (**4a-b**); 250 mM imidazole (**5**); 500 mM imidazole (**6**). Purified ADH-A (38 kD) was collected in fractions **4a-b** and **5**. Fraction **5** was taken for subsequent CD measurements.

YGL157w: cell pellet (**2**); 25 mM imidazole (**3a-b**); 100 mM imidazole (**4**); 250 mM imidazole (**5**); 500 mM imidazole (**6**). YGL157w (38 kD) was collected in fractions **4** and **5**. Fraction **5** was taken for subsequent CD measurements.

LbADH lysate: for evaluation of expression levels, whole cell lysate with overexpressed LbADH (**4**) appearing at 25 kD is shown in comparison to whole cell lysates containing HLADH (**2**) and ADH-A (**3**).

II. CD Spectra of the Substrate-treated Enzymes

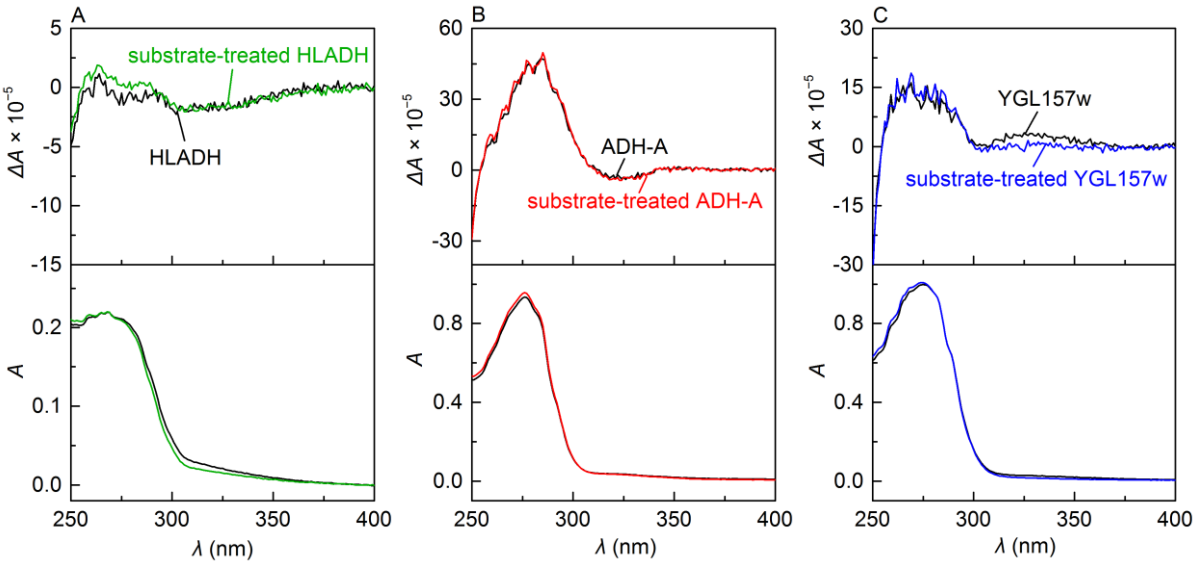

Figure S2. CD and UV-visible absorbance spectra recorded before and after substrate addition. A) HLADH (~6 µM, black). No change of the CD band at λ = 340 nm was observed after addition of 10 mM cyclohexanone (green) B) ADH-A (~15 µM, black). No significant change in the spectra was observed after addition of 10 mM acetone . C) YGL15w (~20 µM, black). After addition of 50 µM ethyl-4-chloroacetoacetate the positive signal at λ = 340 nm decreases slightly (blue).

III. Analysis of NADH Concentration-dependent CD Spectra of HLADH

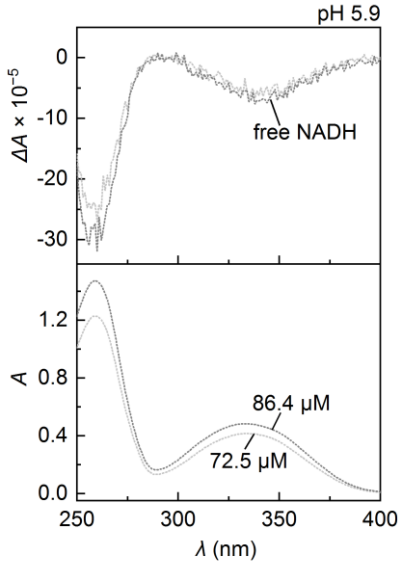

Figure S3. Pure NADH spectra (72.5 and 86.4 µM) recorded at pH 5.9 (MES, 25 mM).

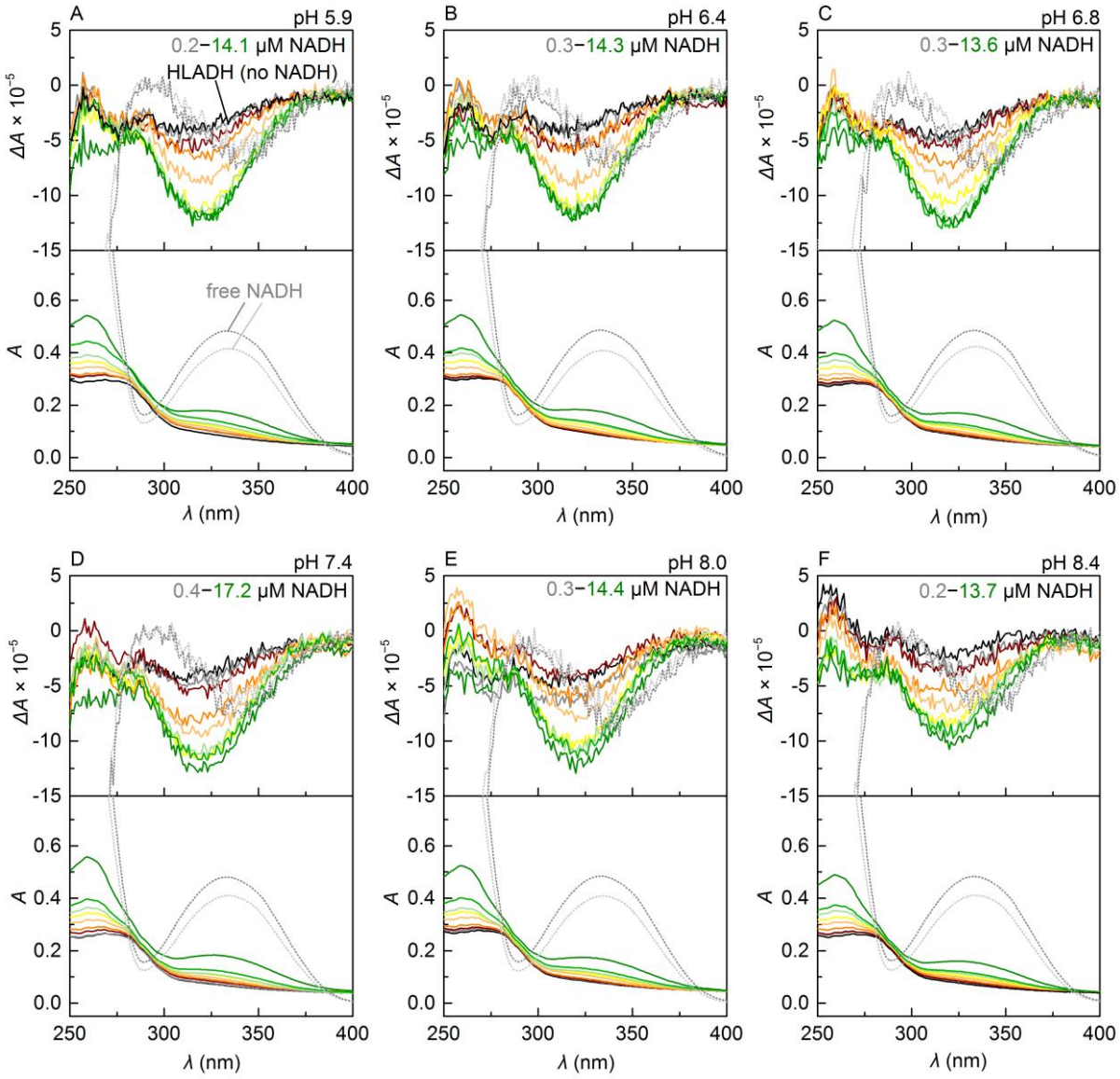

Figure S4. Raw data of the HLADH·NADH complex measured at pH 5.9 (A), 6.4 (B), 6.8 (C), 7.4 (D), 8.0 (E) and 8.4 (F) (shown as coloured compact lines) and spectra of 72 and 86 µM solutions of free NADH (shown as dotted light and dark grey spectra).

Singular Value Decomposition (SVD)

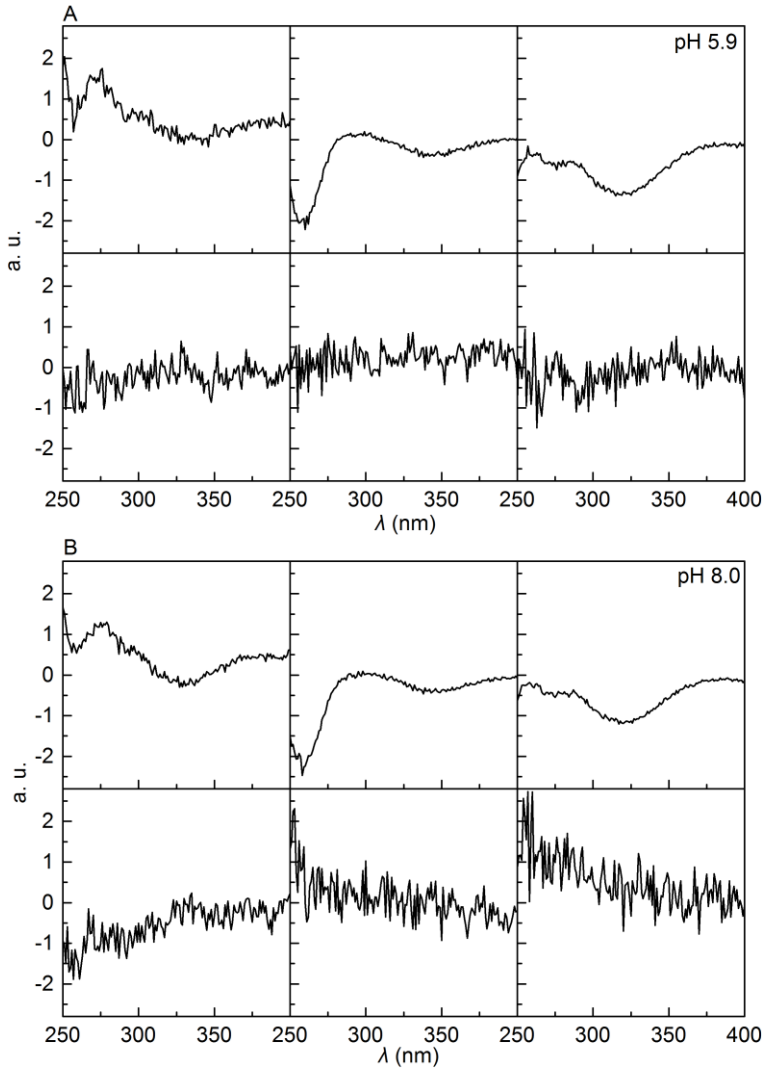

Figure S5. First six orthonormal spectra from SVD of the NADH concentration-dependent CD spectra of HLADH at pH 5.9 (A) and pH 8.0 (B). In agreement with the model, only the first three orthonormal spectra represent real spectral components. All following orthonormal spectra contain only noise and baseline fluctuations (see B, lower panel). To assure a better separation of true signals and baseline fluctuations, SVD has been applied on the first derivative spectra (**A′**) instead of the original spectra (**A**) as suggested by Lórenz-Fonfría and Kandori (see ref. [26]). The orthonormal spectra shown here are back calculated from dividing the data matrix **A** by $\mathbf{S} \times \mathbf{V}^{\mathbf{T}}$ from the SVD on **A′**.

Global Fitting

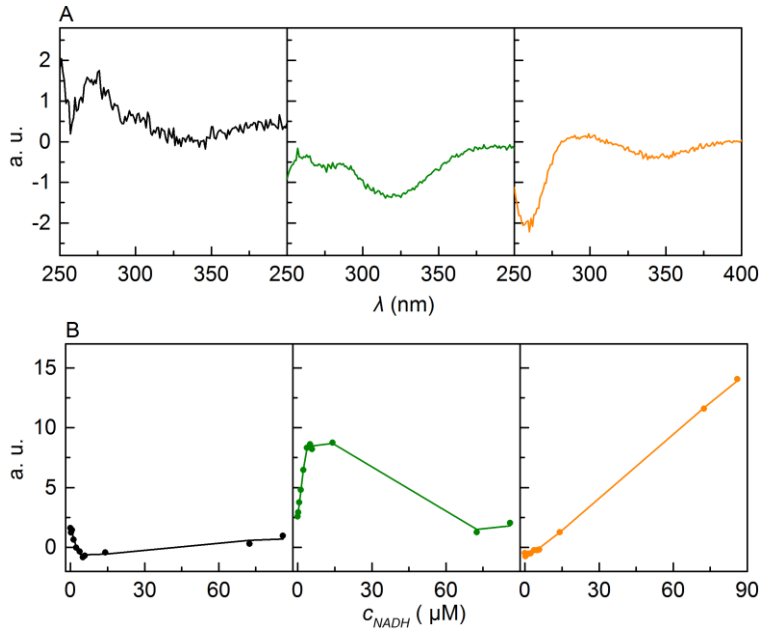

Figure S6. Analysis of the NADH concentration-dependent CD spectra of HLADH (pH 5.9). A) First three orthonormal spectra from Figure S5A. B) Corresponding orthonormal concentration-dependent vectors from SVD containing the coefficients with which the orthonormal spectra contribute to each NADH concentration-dependent spectrum (black, green and orange dots). Lines show the fitting of equation (7) to these coefficients.

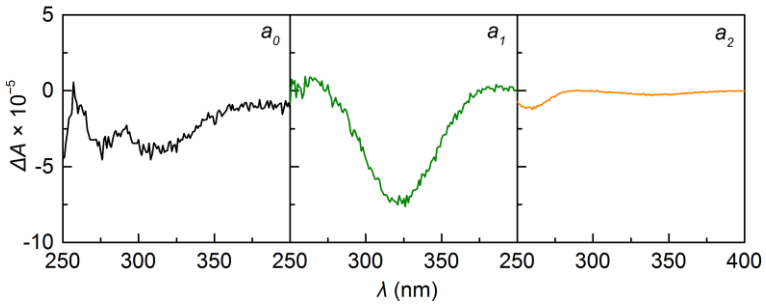

Figure S7. Amplitude spectra a_0, a_1, and a_2 for the NADH-titration of HLADH at pH 5.9 as obtained from multiplication of the data matrix **A** and $\mathbf{F}^{T+}$, the pseudoinverse of a matrix containing the coefficients calculated from equation (7) using the parameters obtained from the fitting as shown in Figure S6 (a_0 is free enzyme spectrum, a_1 is the complex minus free enzyme and minus free cofactor, and a_2 is the free cofactor spectrum). Note that a_0, a_1, and a_2 are not necessarily identical with the first three orthonormal spectra shown in Figure S6A. Owing to the inclusion of the two additional cofactor spectra, amplitude a_2 has the best signal to noise ratio.

Validation

Table S1. Summary of results and confidence criteria for different trials with different constraints[a] for the fitting of NADH concentration-dependent HLADH CD spectra at different pH values.

pH	Entry	K_d (µM)	c_E (µM)	$R \times 10^{-2}$ (stat.)	$R_{SVD} \times 10^{-2}$ (stat.)	s_{HLADH}	s_{NADH}
5.9	***1***	5.96	6.0	7.9 (3.8)	6.3 (1.4)	0.9949	0.0522
	2	0.003	3.3	6.7 (3.9)	4.4 (1.4)	0.9950	0.9349
	3	0.02	3.3	7.2 (4.8)	4.3 (0.6)	0.9950	0.9991
	4	0.04	3.2	7.7 (4.8)	5.5 (0.7)	1.0000	0.9990
6.4	***1***	4.46	6.0	8.8 (4.0)	7.5 (1.6)	0.9933	0.0345
	2	0.09	3.8	8.4 (4.0)	6.9 (1.5)	0.9941	0.9642
	3	0.06	3.9	8.3 (4.6)	5.3 (0.8)	0.9936	0.9988
	4	0.08	3.8	8.3 (4.8)	5.1 (0.7)	1.0000	0.9988
6.8	***1***	6.23	6.0	6.0 (3.8)	4.3 (1.3)	0.9940	-0.0421
	2	0.50	3.4	6.7 (3.8)	4.4 (1.1)	0.9954	0.8112
	3	0.11	3.7	7.7 (4.7)	5.2 (0.7)	0.9944	0.9983
	4	0.14	3.5	8.3 (4.9)	6.4 (0.8)	1.0000	0.9983
7.4	***1***	2.91	6.0	10.8 (3.7)	6.0 (0.8)	0.9892	0.4206
	2	0.30	3.2	9.3 (3.8)	4.2 (0.5)	0.9927	0.9379
	3	0.09	3.6	9.5 (4.6)	6.1 (1.0)	0.9924	0.9988
	4	0.22	3.1	9.3 (4.7)	4.9 (0.9)	1.0000	0.9988
8.0	***1***	6.02	6.0	19.5 (4.1)	16.0 (1.9)	0.9635	0.4165
	2	0.19	2.1	20.6 (4.2)	15.4 (1.4)	0.9907	0.9119
	3	0.31	3.2	16.1 (4.6)	10.3 (1.2)	0.9685	0.9991
	4	0.44	2.6	16.8 (4.7)	11.0 (1.0)	1.0000	0.9990
8.4	***1***	5.97	6.0	12.5 (5.2)	10.4 (2.9)	0.9373	-0.6100
	2	0.54	2.7	10.3 (5.2)	9.6 (2.9)	0.9619	0.2656
	3	1.28	1.9	10.8 (5.8)	6.1 (2.0)	0.9414	0.9985
	4	1.19	1.0	10.7 (6.0)	4.7 (1.0)	1.000	0.9985

[a]Entry 1: c_E is kept fixed (determined from UV-absorbance at $\lambda = 280$ nm); entry 2: c_E is left as an open parameter; entry 3: c_E is left as an open parameter and free NADH spectra are added to the fitting procedure; entry 4: in addition to the conditions in entry 3, amplitude a_0 (free enzyme spectrum) is forced to be identical with *CD* at $c_{rel} = 0$.

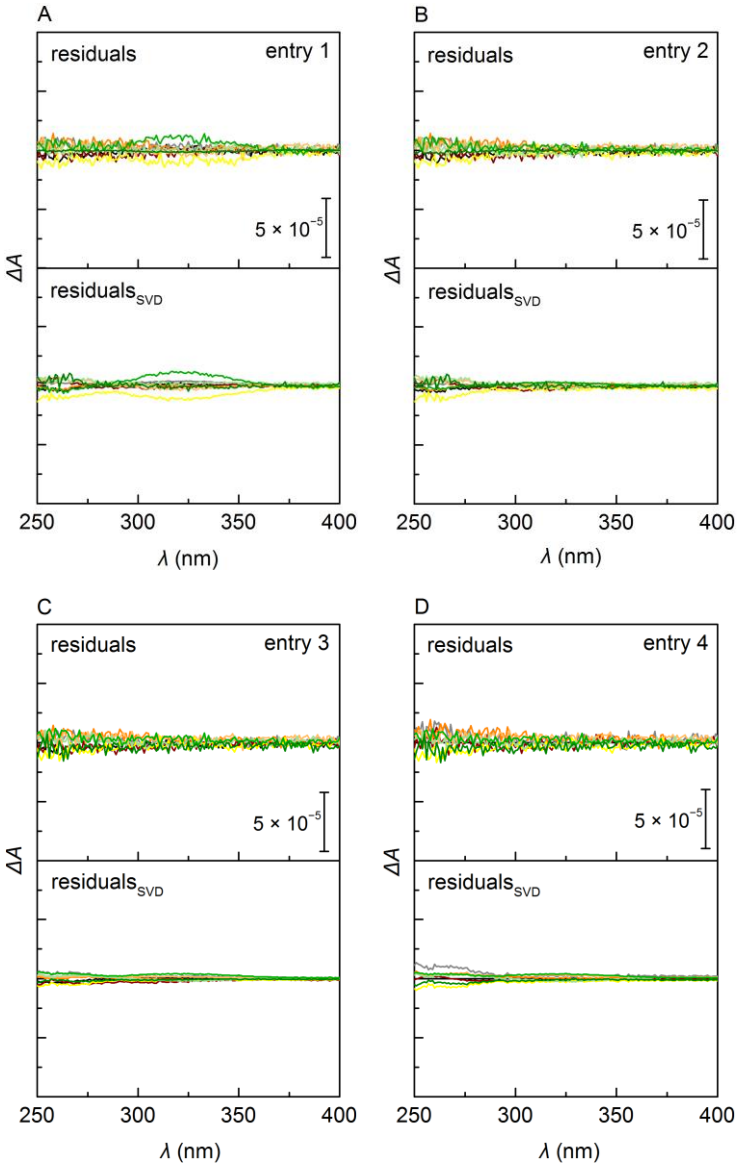

Figure S8. Residuals for the fittings of NADH concentration-dependent HLADH at pH 5.9. The spectra correspond to the entries in Table S1: entry 1 (A), entry 2 (B), entry 3 (C) and entry 4 (D). The upper spectra correspond to the residuals obtained from subtraction of the fitted data from the experimental. The lower spectra correspond to the residuals obtained from subtracting the fitted data from a data set constructed with the first three SVD components from Figure S6. As noise and baseline fluctuations are considerably reduced in this data set, it is easier to detect systematic errors (i. e. true spectral components) in these residuals.

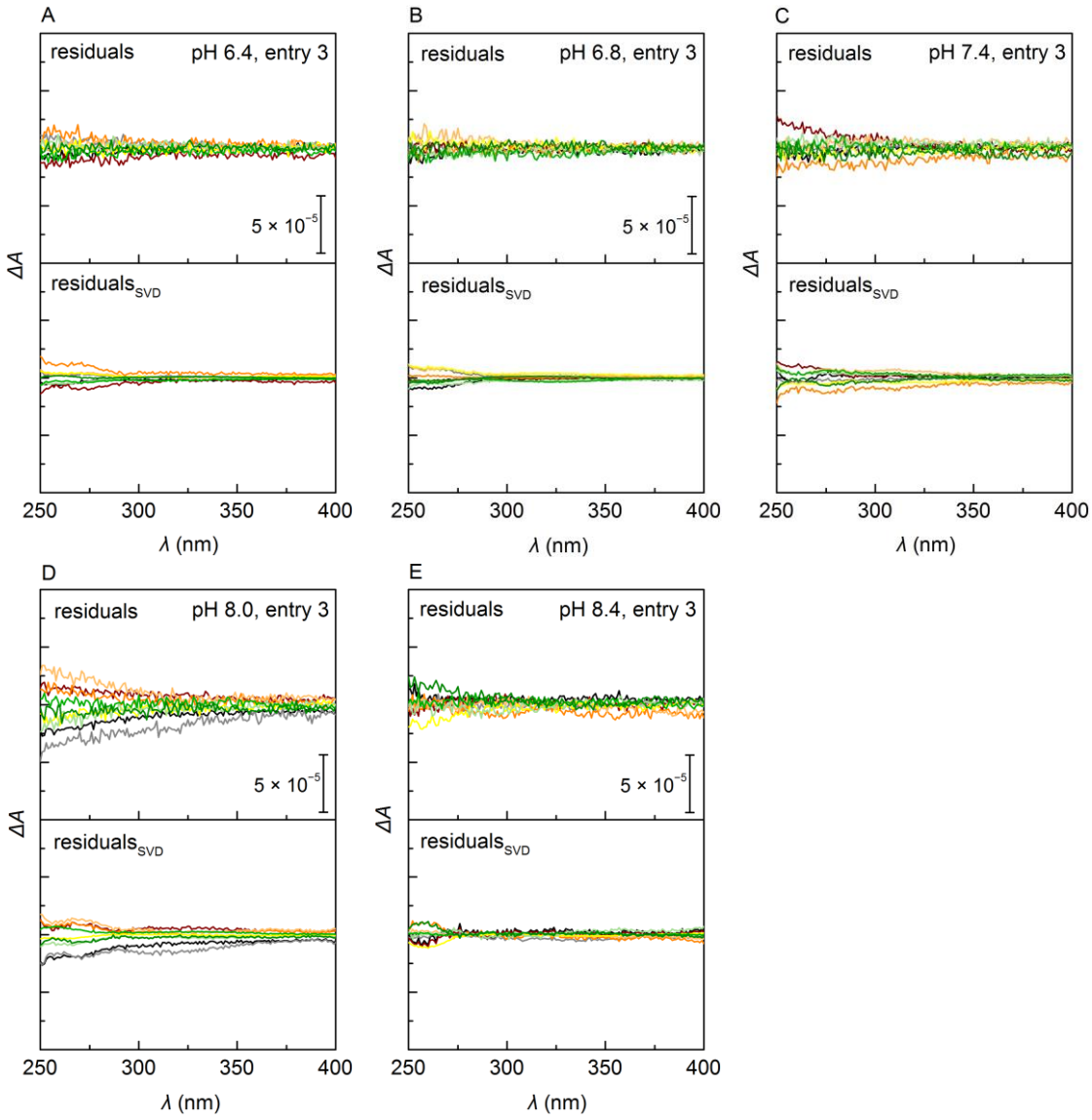

Figure S9. Residuals (upper spectra) and SVD residuals (lower spectra) for the fittings of NADH concentration-dependent HLADH at pH 6.4 (A), 6.8 (B), 7.4 (C), 8.0 (D) and 8.4 (E), each fitted using the parametrization from Table S1, entry 3.

IV. Analysis of NADH Concentration-dependent CD Spectra of HLADH: Influence of Ionic Strength

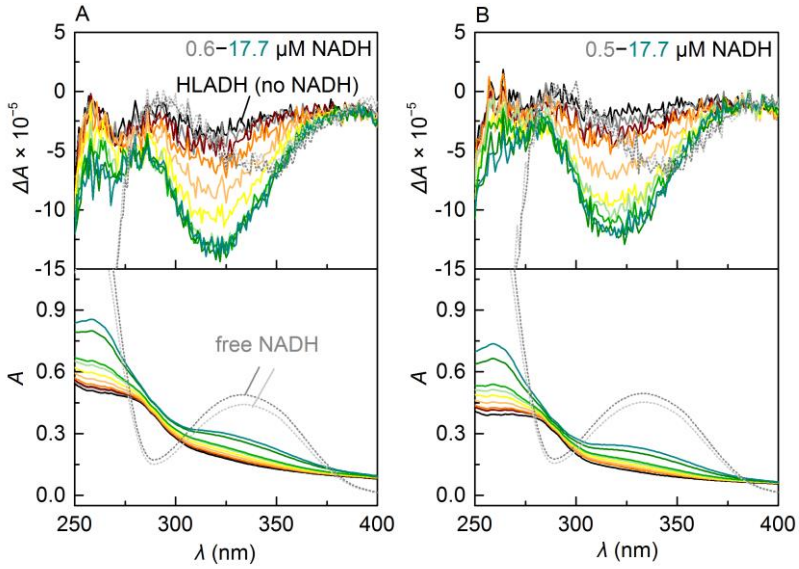

Figure S10. Raw data of the HLADH·NADH complex at pH 6.2 without (A) and with addition of 50 mM NaCl (B). NADH concentration-dependent spectra of HLADH are shown as coloured compact lines; pure NADH spectra are shown as dotted grey lines.

Global Fitting

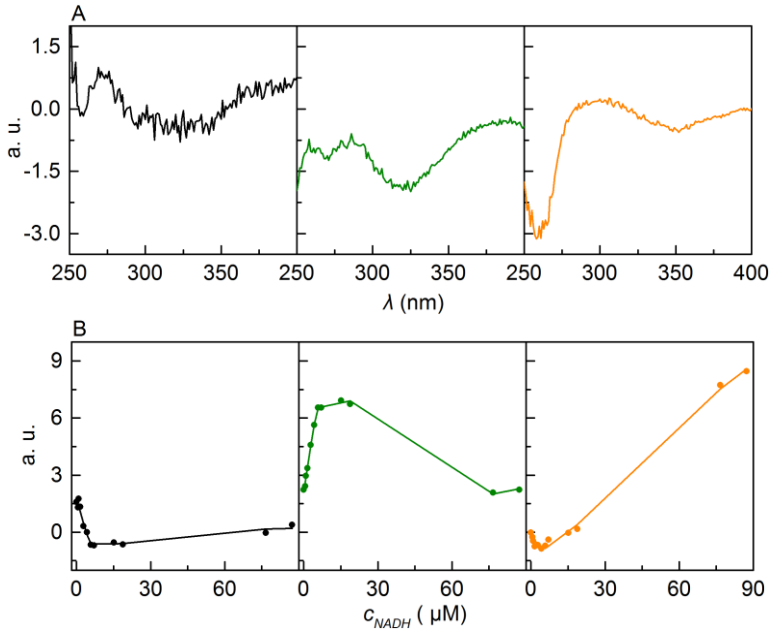

Figure S11. SVD analysis of the HLADH·NADH complex at pH 6.2 without added NaCl. A) First three orthonormal spectra. B) Corresponding coefficients and fits of equation (7).

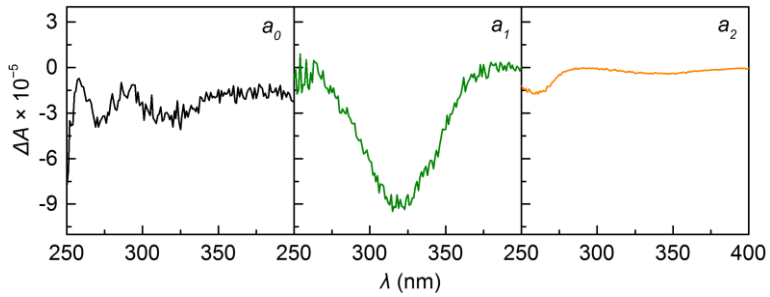

Figure S12. Amplitude spectra for NADH-titration of HLADH at pH 6.2 according to equation (7) (compare Figure S7).

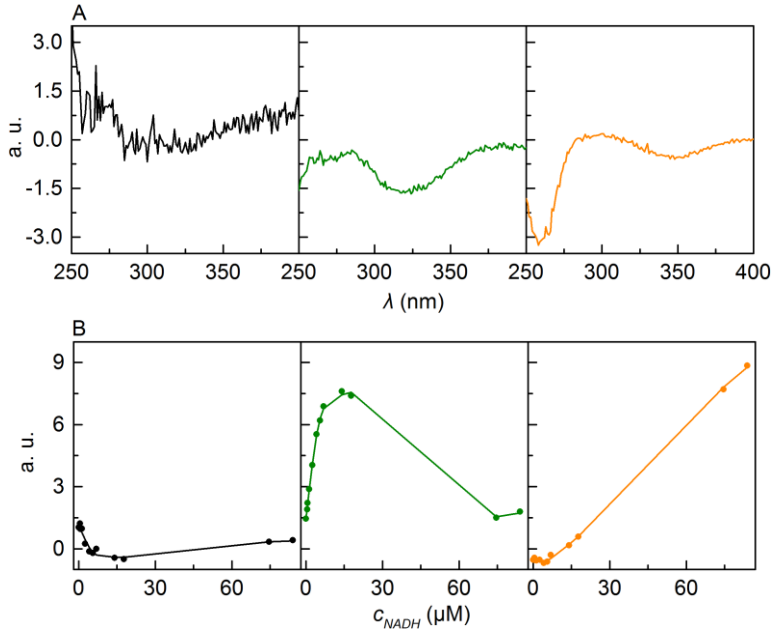

Figure S13. SVD analysis of the HLADH·NADH complex at pH 6.2 in presence of 50 mM NaCl. A) First three orthonormal spectra. B) Corresponding coefficients and fits of equation (7).

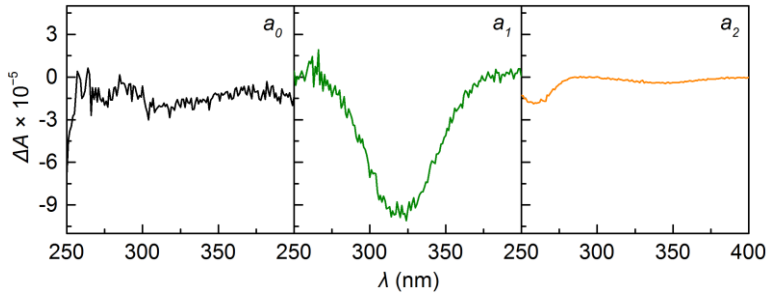

Figure S14. Amplitude spectra for NADH-titration of HLADH at pH 6.2 in presence of 50 mM NaCl according to equation (7). While addition of salt increases the K_d of the HLADH·NADH complex, the overall appearance of the amplitude spectra is not significantly affected in comparison to the salt-free experiment shown in Figure S12.

Validation

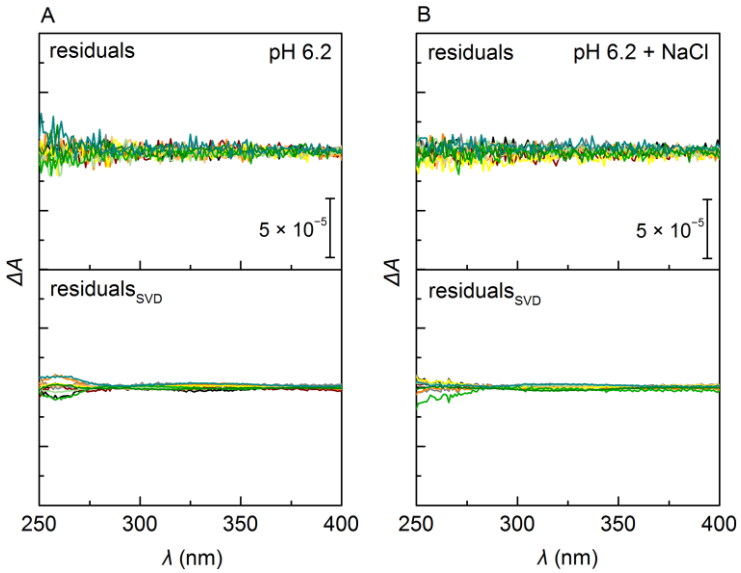

Figure S15. Residuals (upper spectra) and SVD residuals (lower spectra) for the fittings of NADH concentration-dependent HLADH spectra at pH 6.2, without (A) and with addition of NaCl (B).

V. Analysis of the ADH-A·NADH Complex

Global Fitting

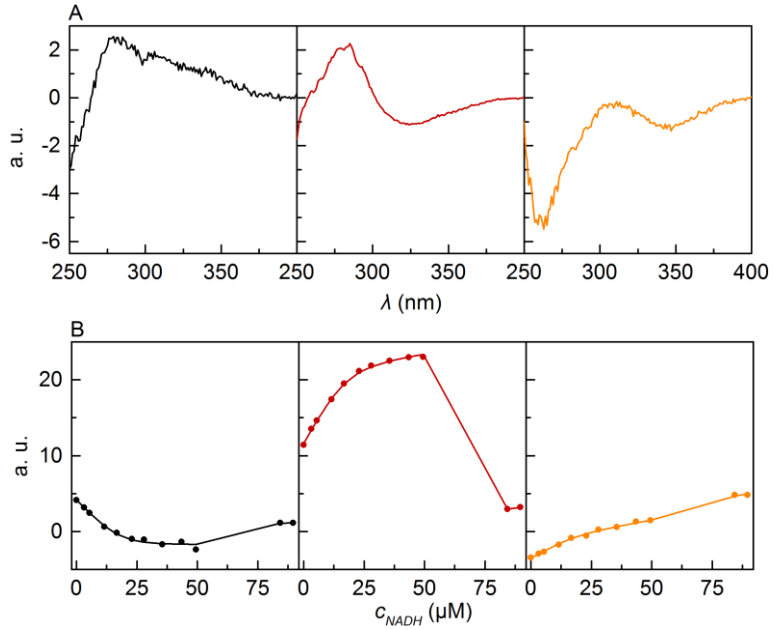

Figure S16. SVD analysis of the CD spectra from the NADH-titration of ADH-A. A) First three orthonormal spectra. B) Corresponding coefficients and fits of equation (7).

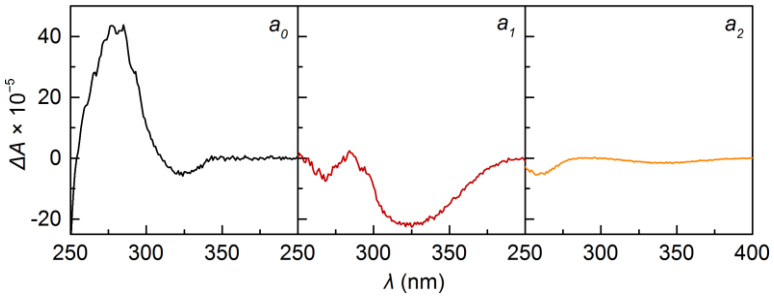

Figure S17. Amplitude spectra for the NADH-titration of ADH-A according to equation (7).

Validation

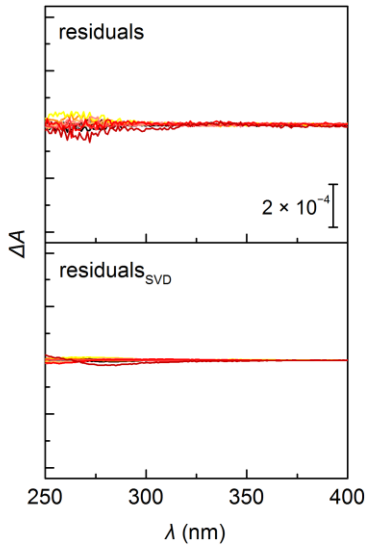

Figure S18. Residuals (upper spectra) and SVD residuals (lower spectra) for the fittings of NADH concentration-dependent ADH-A spectra.

VI. Analysis of the YGL157w·NADPH Complex

Global Fitting

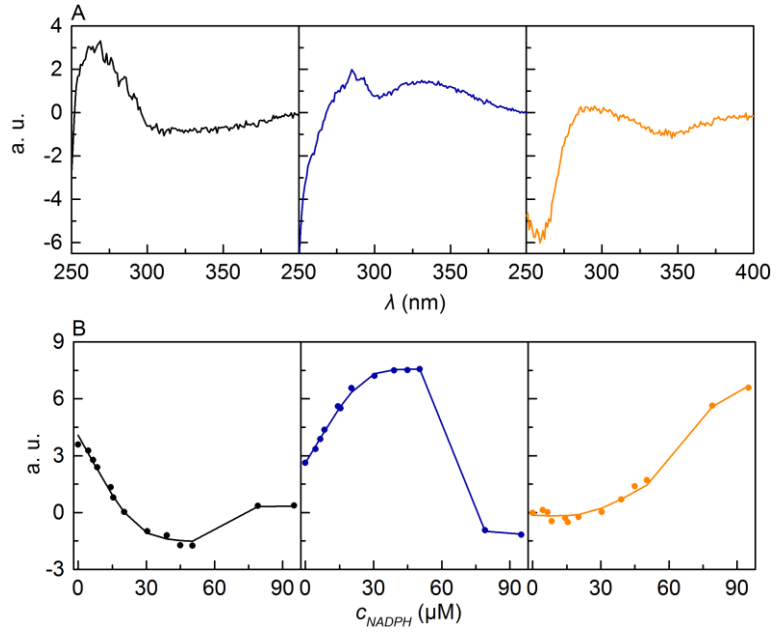

Figure S19. SVD analysis of the CD spectra from the NADPH-titration of YGL157w. A) First three orthonormal spectra. B) Corresponding coefficients and fits of equation (7).

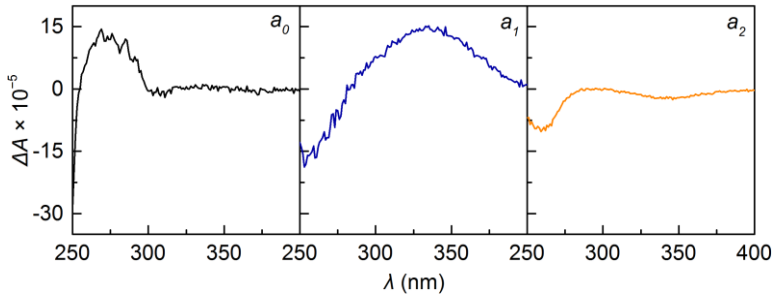

Figure S20. Amplitude spectra for the NADPH-titration of YGL157w according to equation (7). Note that the amplitude associated with formation of the YGL157w·NADPH complex (a_1) has an opposite sign in comparison to the corresponding a_1 determined for the HLADH·NADH and the ADH-A·NADH complex.

Validation

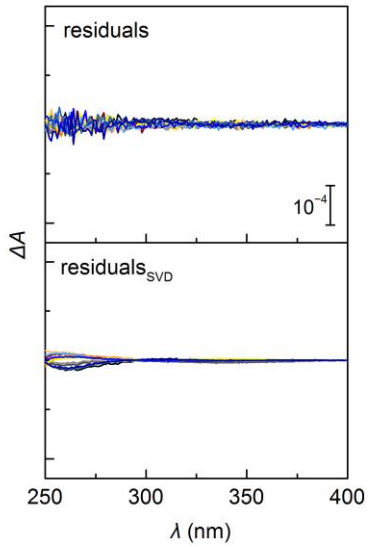

Figure S21. Residuals (upper spectra) and SVD residuals (lower spectra) for the fittings of NADPH concentration-dependent YGL157w spectra.

VII. Analysis of the LbADH·NADPH Complex

Global Fitting

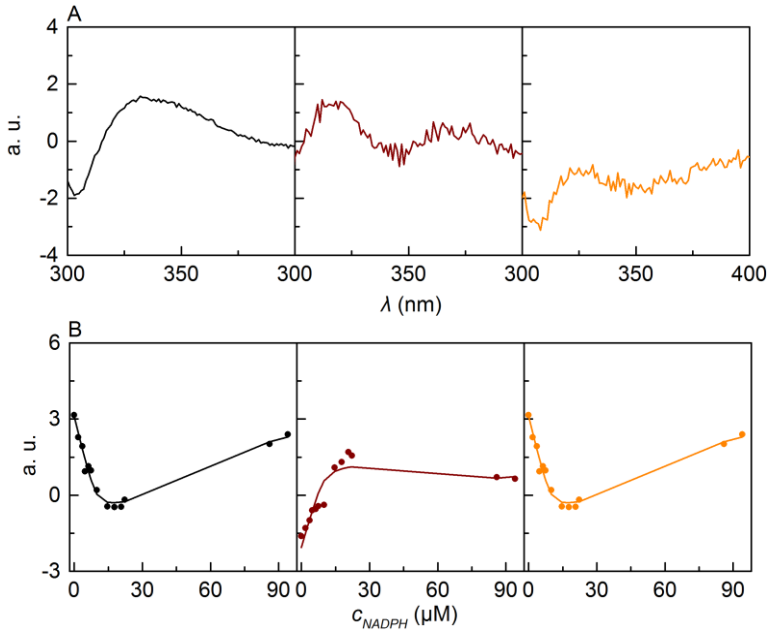

Figure S22. SVD analysis of the CD spectra from the NADPH-titration of LbADH lysate. A) First three orthonormal spectra. B) Corresponding coefficients and fits of equation (7).

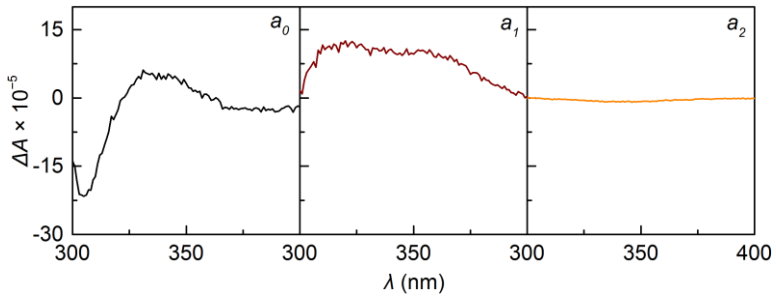

Figure S23. Amplitude spectra for the NADPH-titration of LbADH according to equation (7). The amplitude associated with formation of the LbADH·NADPH complex (a_1) has a positive sign, similarly as observed with YGL157w·NADPH complex (Figure S20).

Validation

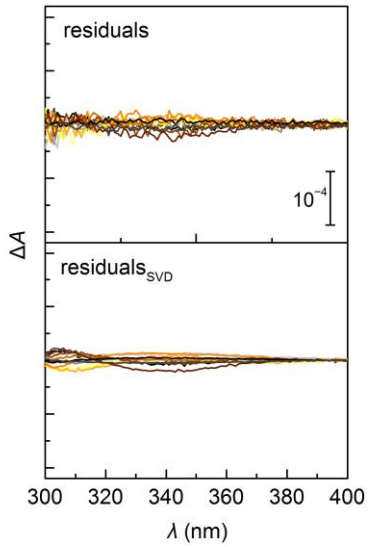

Figure S24. Residuals (upper spectra) and SVD residuals (lower spectra) for the fittings of NADPH concentration-dependent LbADH spectra.

VIII. Quantum Chemical Calculations of ECD and UV/Vis Spectra

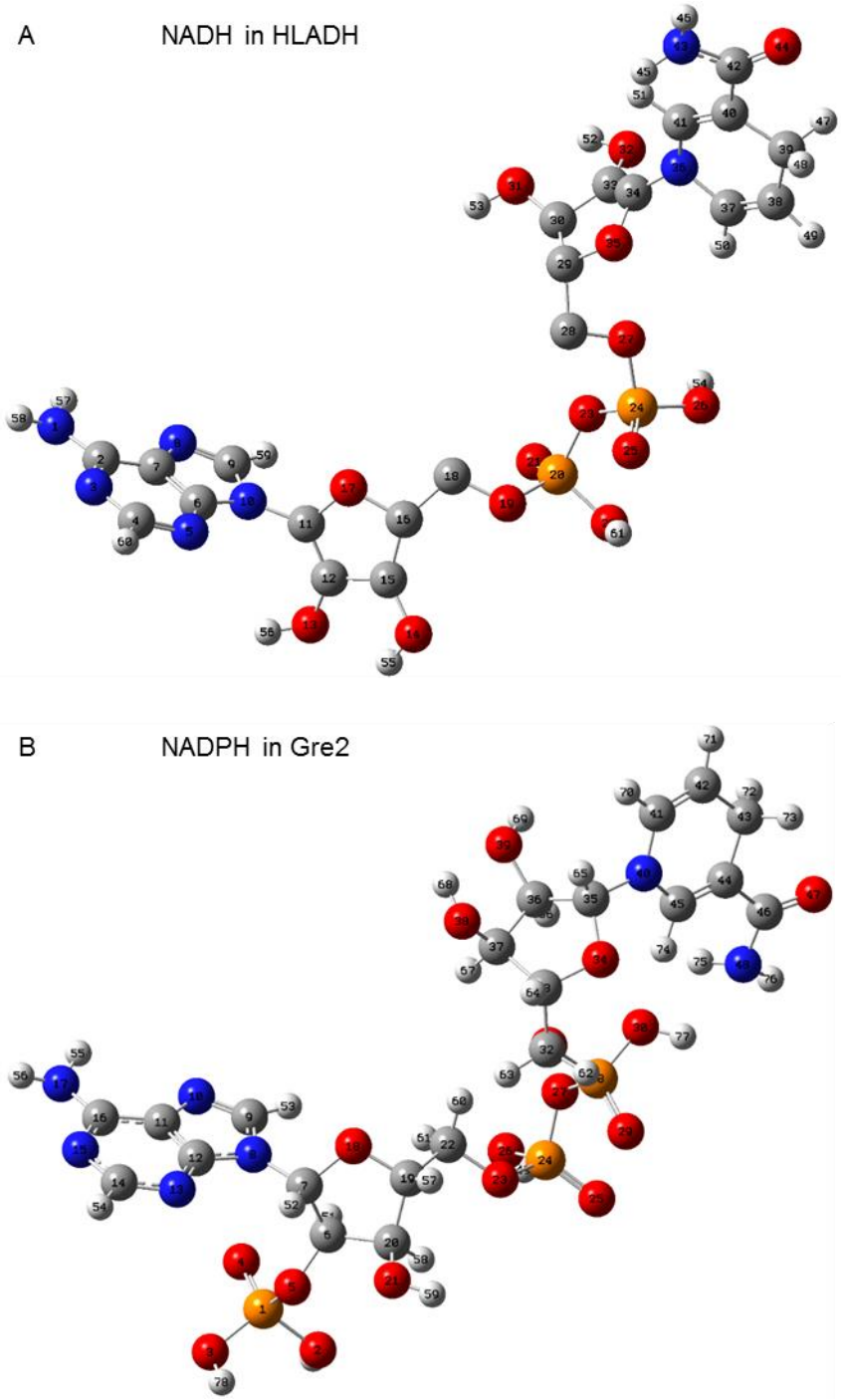

Figure S25. NADH conformation as bound to HLADH[1] (A) and NADPH bound to Gre2[2] (B). The atom numbering is the same for NADH in HLADH or ADH-A, and for NADPH in Gre2 and LbADH, respectively.

Table S2. Constrained atoms (numbering according to Figure S25) of NAD(P)H cofactor geometries from crystal structures of HLADH,[1] ADH-A,[3] Gre2[2] and LbADH[4] used for the calculation of theoretical CD and UV/Vis absorbance spectra.

Enzyme	HLADH	ADH-A	Gre2	LbADH
PDB ID	4XD2[1]	2XAA[3]	4PVD[2]	1ZK4[4]
Constrained Atoms	3 5 13 14 18 21 25 26 28 31 32 36 38 43 44	3 5 13 14 18 22 25 26 28 31 32 36 38 43 44	2 3 4 11 12 15 17 21 22 25 29 38 39 42 44 47 48	3 4 15 17 21 22 29 30 32 38 39 42 47

Table S3. Wavelength and bandwidth corrections for the calculated UV/Vis and ECD spectra of the bound NAD(P)H cofactor in the four studied enzymes.

Enzyme	**Wavelength correction (nm)**	**Bandwidth (eV)**
HLADH	+12	0.30
ADH-A	+38	0.30
Gre2	+23	0.45
LbADH	+22	0.45

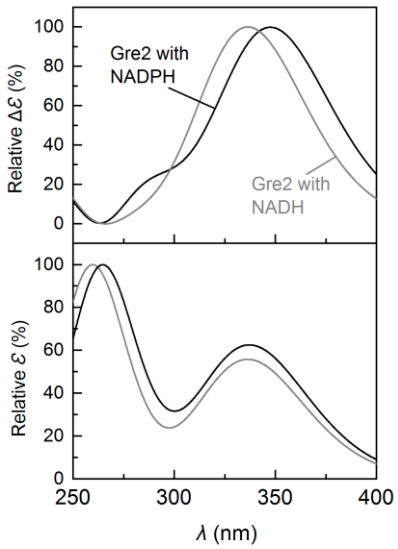

Figure S26. Theoretical CD and UV/Vis spectra for NADPH and NADH bound to Gre2, calculated at sTD-DFT level.[5] The phosphate group on the ribose of adenosine in NADPH was removed, the constraints for the calculations of NADH were the same as for NADPH (Table S2). The removal of the phosphate does not change the sign of the CD band 300 and 400 nm.

IX. Activity of HLADH at different pH

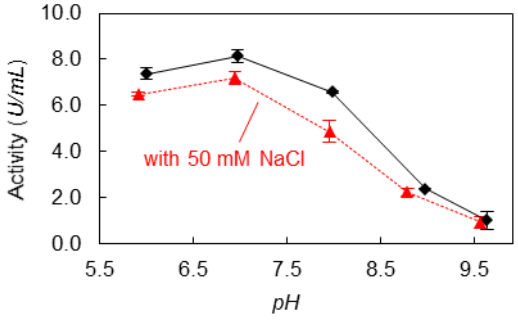

Figure S27: pH-dependence of HLADH catalytic activity for the reduction of cyclohexanone without (black compact line) and with added NaCl (red dotted line). The activity was determined photometrically by monitoring the time-dependent decrease of NADH absorbance at λ = 340 nm with a UV 1650 PC spectrophotometer (Shimadzu, Kyoto, Japan) at room temperature for 60 s (substrate concentration: 10 mM; cofactor concentration: 250 µM). The reaction was started by addition of 10 µL of diluted enzyme solution (final volume: 1 mL). The activity was calculated as enzyme units (1 U = 1 µmol substrate conversion per minute) with a molecular extinction coefficient for NADH ($\varepsilon_{340\ nm}$) of 6.2 $\mu mol^{-1}\ cm^{-1}$.[6] Each data point was measured in triplicate. The catalytic activity of HLADH decreases with higher pH. Addition of 50 mM NaCl reduces the activity throughout the assayed pH range.

X. References

1. S. Ramaswamy, M. Scholze and B. V. Plapp, *Biochemistry*, 1997, **36**, 3522–3527.
2. P.-C. Guo, Z.-Z. Bao, X.-X. Ma, Q. Xia and W.-F. Li, *Biochim. Biophys. Acta*, 2014, **1844**, 1486–1492.
3. M. Karabec, A. Łyskowski, K. C. Tauber, G. Steinkellner, W. Kroutil, G. Grogan and K. Gruber, *Chem. Commun.*, 2010, **46**, 6314–6316.
4. N. H. Schlieben, K. Niefind, J. Müller, B. Riebel, W. Hummel and D. Schomburg, *J. Mol. Biol.*, 2005, **349**, 801–813.
5. C. Bannwarth and S. Grimme, *Comput. Theor. Chem.*, 2014, **1040-1041**, 45–53.
6. J. Ziegenhorn, M. Senn and T. Bücher, *Clin. Chem.*, 1976, **22**, 151–160.